

Cosmic-Dawn 21-cm Signal from Dynamical Dark Energy

Lu Yin^{1*}

¹*Asia Pacific Center for Theoretical Physics, Pohang, 37673, Korea*

The 21-cm signal is the most important measurement for us to understand physics during cosmic dawn. It is the key for us to understand the expansion history of the Universe and the nature of dark energy. In this paper, we focused on the characteristic 21-cm power spectrum of a special dynamic dark energy - the Interacting Chevallier-Polarski-Linder (ICPL) model - and compared it with those of the Λ CDM and CPL models. From the expected noise of HERA, we found more precise experiments in the future can detect the features of interacting dark energy in the 21-cm power spectra. By studying the brightness temperature, we found the ICPL model is closer to the observation of EDGES compared to the Λ CDM, thus alleviating the tension between theory and experiments.

I. INTRODUCTION

The Experiment to Detect the Global Epoch of Reionization Signature (EDGES) has reported the detection of an absorption profile centered at 78 MHz [1], corresponding to a redshift $z \approx 17$, which is named the global 21-cm signal. The 21-cm signal refers to the wavelength of the electromagnetic radiation emitted by neutral hydrogen atoms at cosmic dawn. Specifically, it corresponds to the transition between the two hyperfine energy levels of the hydrogen atom, where the electron's spin and the proton's spin are aligned (parallel) and anti-aligned (anti-parallel) with each other [2–4]. The global 21-cm signal provides valuable information about the distribution and properties of neutral hydrogen gas in the Universe. It is particularly significant for studying the epoch of reionization, the formation of the first galaxies and stars, and the large-scale structure of the Universe [5–18]. However, the amplitude of the absorption profile reported by EDGES is more than twice the maximum allowed in the standard cosmological evolution, which implies the new physics beyond the standard model [1].

To generate a possible strong signal in the 21-cm line, two mechanisms are commonly considered. The first mechanism involves enhancing the background radiation temperature through processes such as dark matter decay or annihilation [19–23]. These models propose that the presence of additional energy injected into the system leads to an increase in the background radiation temperature, which in turn affects the 21-cm signal. The second mechanism focuses on lowering the gas temperature through interactions between dark matter and baryons [7, 24–28]. By considering elastic scattering or other interactions between these particles, the thermal state of the gas can be modified, resulting in a different 21-cm signal. However, many existing theories face challenges when confronted with other astronomical observations. People are looking forward to a model involving additional cooling or heating mechanisms to solve this tension.

The interactions between dark matter and dark energy can influence the gas temperature and, consequently, the 21-cm signal [29–32]. On the one hand, interacting dark energy (IDE) can be fitted with other observations well and can give different 21-cm predictions. On the other hand, the 21-cm signal will help to constrain the equation of state of dark energy and distinguish dark energy models. In this work, we consider the phenomenology of 21-cm global signal for two special dynamical dark energy models: the Chevallier-Polarski-Linder (CPL) model [33–35] and the Interacting CPL (ICPL) model [36]. We will compare the difference in the 21-cm global signal with the Λ CDM by using the star-formation rate density (SFRD) method from the *Zeus21* program [37].

Except EDGES, there are other 21-cm observations, such as the Shaped Antenna measurement of the background Radio Spectrum (SARAS)[38], the Large-aperture Experiment to Detect the Dark Ages (LEDA) [39], the Low-Frequency Array (LOFAR)[40], the Murchison Widefield Array (MWA)[41, 42], the Hydrogen Epoch of Reionization Array (HERA)[43, 44], and the upcoming Square Kilometre Array (SKA) [45–49]. We will also compare our theoretical model predictions with the HERA data by imploring the expected noise.

The paper will proceed as follows. We review the calculation of 21-cm brightness temperature in

*Electronic address: lu.yin@apctp.org

Section II. And Section III shows the background evolution of the CPL, the ICPL, and the Λ CDM model with their best-fit results in local observations. In Section IV, we calculate the 21-cm brightness temperature signals from the three models. Moreover, we compare the power spectra of the three models with the expected noise from HERA. The conclusion is presented in Section V.

II. 21-CM LINE BRIGHTNESS TEMPERATURE

The 21-cm line is produced when the electron and proton in a hydrogen atom are in opposite spin states, which is known as hyperfine splitting. When the electron and proton flip their spins and move to the other spin state, they emit or absorb a photon with a frequency of about 1420 MHz, corresponding to a wavelength of 21 cm. The brightness temperature T_{21} is defined as the temperature an observer would measure from a 21-cm line observation and describes the strength of the global sky-average signal, which can be given by:

$$T_{21} = \frac{T_S - T_{\text{CMB}}}{1+z} (1 - e^{-\tau_{21}}), \quad (1)$$

where T_S is the spin temperature of the hydrogen atom, T_{CMB} is the temperature of the cosmic microwave background radiation, and z is the redshift of the observed 21-cm line. The spin temperature is a measure of the population difference between the two hyperfine energy levels of the hydrogen atom, and it depends on the collisional and radiative processes.

The τ_{21} represents the 21-cm optical depth of the diffuse intergalactic medium [50] and can be calculated as

$$\tau_{21} = (1 + \delta) x_{\text{HI}} \frac{T_0}{T_S} \frac{H(z)}{\partial_r v_r} (1 + z), \quad (2)$$

where x_{HI} is the fraction of neutral hydrogen, δ is the density of the neutral hydrogens, $H(z)$ is the Hubble parameter, and $\partial_r v_r$ is the velocity line-of-sight gradient. The normalization factor T_0 can be defined by

$$T_0 = 34\text{mK} \times \left(\frac{1+z}{16}\right)^{1/2} \left(\frac{\Omega_b h^2}{0.022}\right) \left(\frac{\Omega_m h^2}{0.14}\right)^{-1/2}, \quad (3)$$

where the Ω_m and Ω_b are the fractions of the critical density for cold dark matter and baryonic matter. Another important parameter is the color temperature T_c , which is closely associated with the gas kinetic temperature T_k [51] and numerically approximated by

$$T_c \approx T_k^{-1} + g_{\text{col}} T_k^{-1} (T_S^{-1} - T_k^{-1}), \quad (4)$$

where $g_{\text{col}} \approx 0.4055 K$. By taking the approximation $\tau_{21} \ll 1$ [52, 53], we can re-write the 21-cm brightness temperature

$$T_{21} = T_0(z)(1 + \delta - \delta_v) \left(\frac{x_\alpha}{1 + x_\alpha}\right) \left(1 - \frac{T_{\text{CMB}}}{T_c}\right) x_{\text{HI}}, \quad (5)$$

where x_α is the dimensionless Wonhuysen-Field (WF) coupling parameter [37, 54]. Thus, the equation for the 21-cm signal, T_{21} , separates into four different parts. These are: (i) $(1 + \delta - \delta_v)$ represents the large-scale structure, which is described by the local density and velocity fields. (ii) $(x_\alpha/(1 + x_\alpha))$ is the term of the WF effect, which measures the Lyman-alpha emission from the first galaxies. (iii) The term $(1 - T_{\text{CMB}}/T_c)$ can be considered by the gas kinetic and color temperature, which is determined by the competition between adiabatic cooling and X-ray heating due to the first stars. (iv) Reionization is represented by the term x_{HI} . By considering the four terms, the 21-cm signal can be used as a powerful tracer of the formation of the first stars and galaxies, as well as the evolution of the cosmic web at high redshifts.

For cosmic dawn, the recombination process had already finished, and the neutral hydrogen number density had already been set. Therefore, the brightness temperature can be modified via a different background evolution. The dynamical dark energy models will provide a different evolution of Hubble parameter in our Universe and change the T_{21} .

Table I: The background evolution calculated from the Λ CDM, the CPL, and the ICPL model, respectively.

Parameter	Λ CDM	CPL	ICPL
$\omega(z)$	-1	$\omega_0 + \omega_a z/(1+z)$	$\omega_0 + \omega_a z/(1+z)$
Q	0	0	$3\gamma H \rho_c$
ρ_{de}	ρ_{de}^0	$\rho_{de}^0 (1+z)^{3(1+\omega_0+\omega_a)} e^{-\frac{3\omega_a z}{1+z}}$	Eq.11
ρ_c	$\rho_c^0 (1+z)^3$	$\rho_c^0 (1+z)^3$	$\rho_c^0 (1+z)^{3(1-\gamma)}$

III. EVOLUTION OF DYNAMICAL DARK ENERGY MODELS

Based on the FRW Universe, each component of the Universe can be written in Friedmann equations as

$$3M_p^2 H^2 = \rho_r + \rho_b + \rho_c + \rho_{de}, \quad (6)$$

where the energy density of radiation, baryon, cold dark matter, and dark energy can be expressed as ρ_r , ρ_b , ρ_c , and ρ_{de} , respectively. In the local Universe, dark energy and dark matter make up approximately 96% components of the Universe. The change in their energy densities will lead to a different evolutionary history of our Universe.

The ratio between pressure and energy density is the equation of state ($\omega = P/\rho$). In the Λ CDM, ω_{de} is considered as a constant number and equal to -1. But in dynamic dark energy, the equation of state can be evolved with redshift. For example, in Chevallier-Polarski-Linder (CPL) model[33–35], the ω_{de} can be written as

$$\omega_{de} = \omega_0 + \omega_a z/(1+z) = \omega_0 + \omega_a (1-a). \quad (7)$$

If ω_a returns to 0 and ω_0 is -1, this model will go back to the Λ CDM.

The period of cosmic dawn is matter dominated. The interacting dark energy model is one option to change the background evolution during this time and change the thermal history. We consider a special model that has energy transformation between dark energy and dark matter based on CPL, named the ICPL model. Their continuity equation for the energy densities can be parameterized as

$$\begin{aligned} \dot{\rho}_c + 3H\rho_c &= Q, \\ \dot{\rho}_{de} + 3H(1 + w_{de})\rho_{de} &= -Q, \end{aligned} \quad (8)$$

where Q is the non-gravitational interacting energy transfer term. There are already many studies on different forms of Q [32, 36, 55–62]. In this study, we consider Q as

$$Q = 3\gamma H \rho_c, \quad (9)$$

where the γ is the interaction parameter, and we will fit it later. If the value of γ comes back to zero, there is no interaction between dark energy and dark matter anymore, and the model will return to the CPL model. With the energy transfer as Eq. (9), the evolution of cold dark matter and dark energy can be modified as

$$\rho_c = \rho_c^0 (1+z)^{3(1-\gamma)}, \quad (10)$$

$$\begin{aligned} \rho_{de} = & 3\gamma \rho_c^0 (1+z)^{3(1+\omega_0+\omega_a)} e^{3\omega_a/(1+z)} \int_0^z e^{-3\omega_a/(1+z)} (1+z)^{-3(\omega_0+\omega_a+\gamma)-1} dz \\ & + \rho_{de}^0 (1+z)^{3(1+\omega_0+\omega_a)} e^{-3\omega_a z/(1+z)}. \end{aligned} \quad (11)$$

The definitions of the three models in background evolution are summarized in Tab. I. Next, we will use the Markov Chain Monte Carlo (MCMC) to get the best-fit value of every parameter for the three models and discuss their effects on the 21-cm signal.

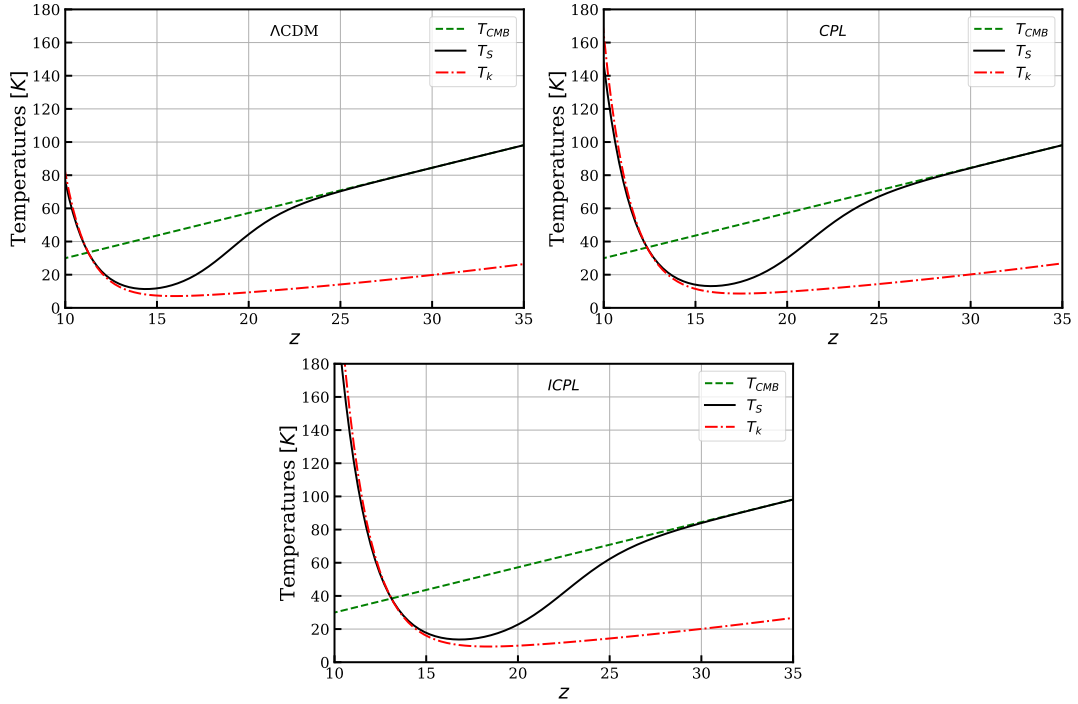


Figure 1: The evolution of the CMB temperature T_{CMB} (dash green line), spin temperature T_S (black line), gas kinetic temperature T_k (dash red line) with redshift in the Λ CDM, the CPL, and the ICPL model.

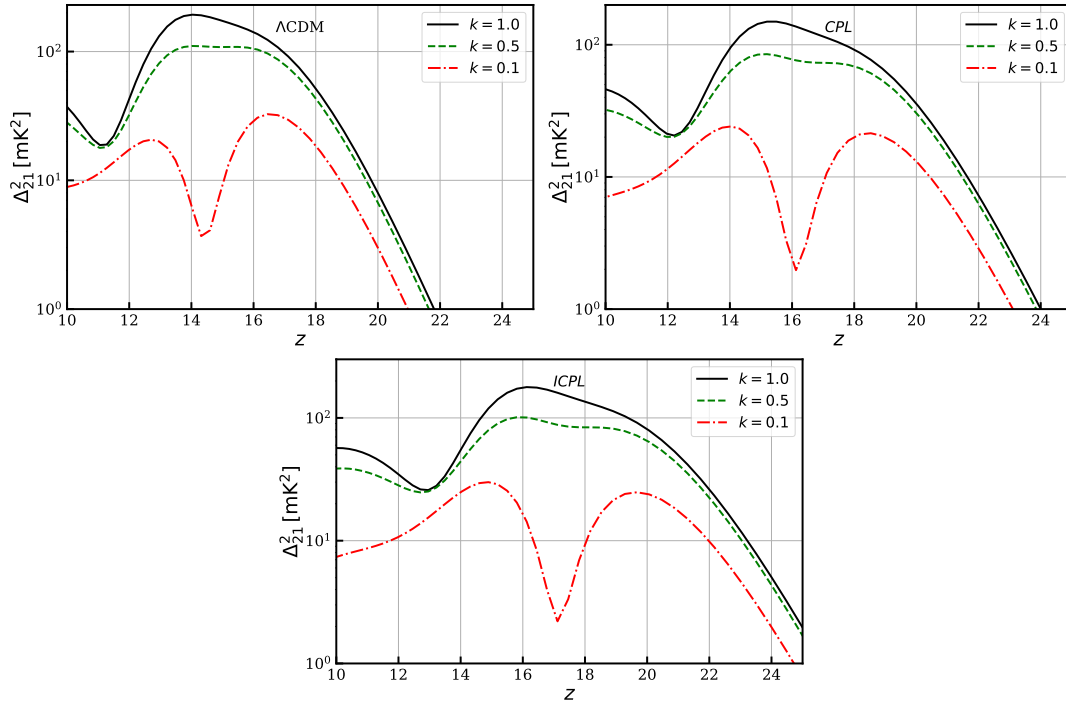


Figure 2: The evolution of 21-cm power spectra with redshift in the CPL, the ICPL, and the Λ CDM. The wave numbers k in the three models are set as 1.0 (black line), 0.5 (dash green line), and 0.1 (dash red line), respectively.

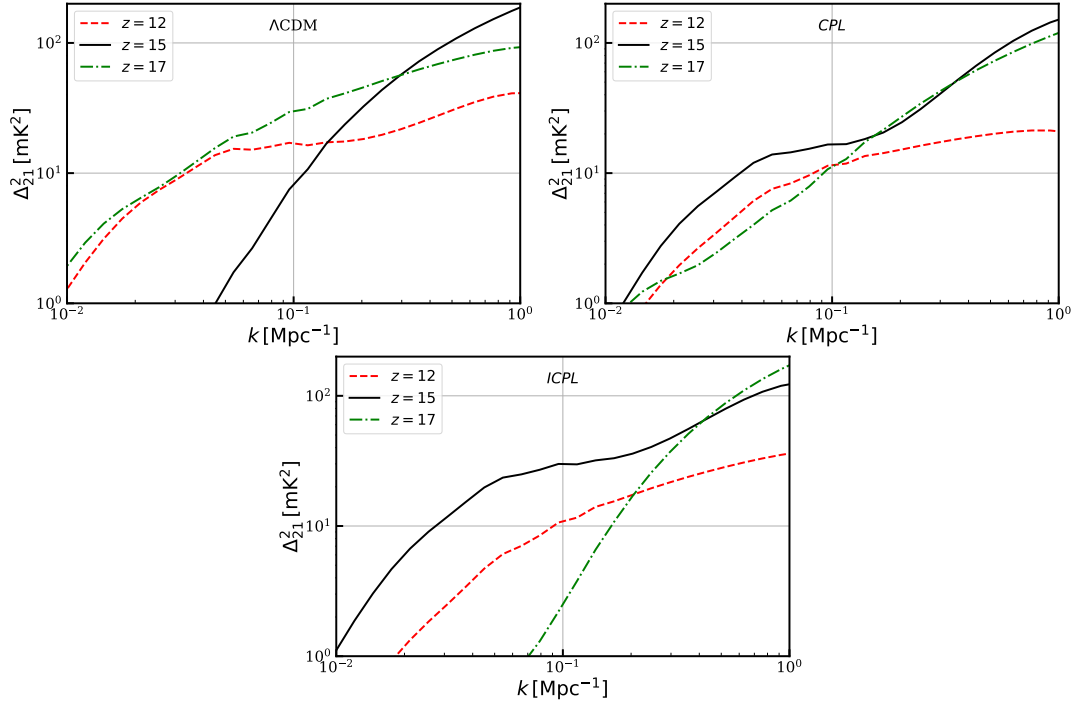


Figure 3: The evolution of 21-cm power spectra in the Λ CDM, the CPL, and the ICPL model. The slices of redshift are selected at 12 (red dash line), 15 (black line), and 17 (green dash line), respectively.

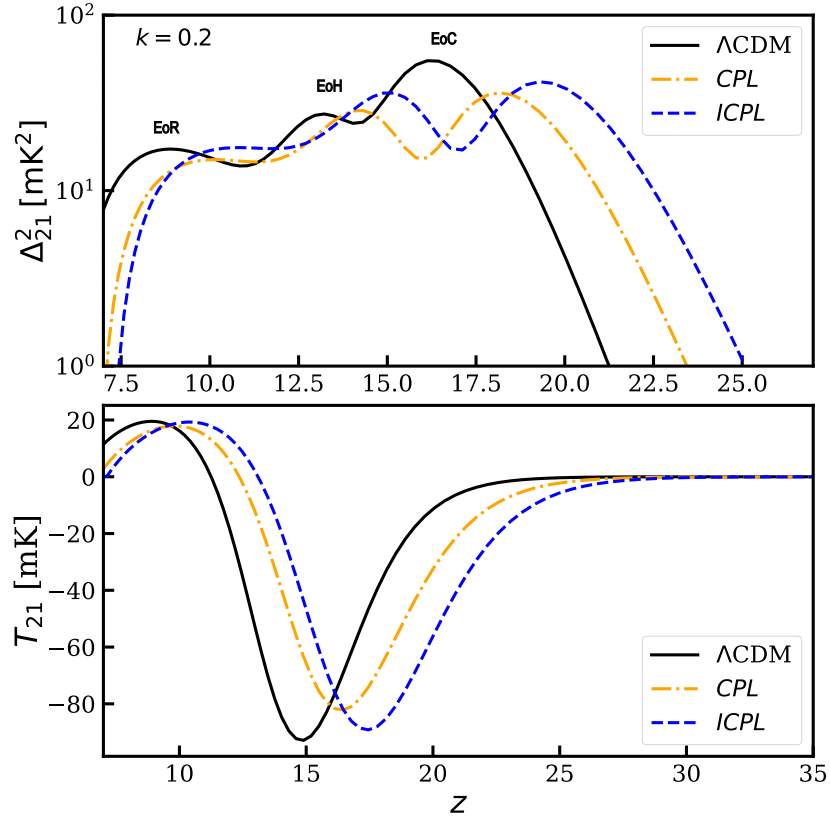


Figure 4: The power spectra (Δ_{21}^2) and brightness temperature (T_{21}) of the 21-cm signal. The theoretical value of the Λ CDM, the CPL, and the ICPL models are shown in the black line, yellow-dash line, and blue-dash line, respectively. In this figure, the wave number k is 0.2.

Table II: The best-fit of free parameters comes from the Λ CDM, the CPL, and the ICPL model, respectively. These results were obtained with 68% C.L. based on the observation of BAO and Type Ia Supernova.

Parameter	Λ CDM	CPL	ICPL
H_0	$69.9182^{+0.1398}_{-0.1369}$	$70.6986^{+0.2639}_{-0.2601}$	$70.9338^{+0.2549}_{-0.2515}$
Ω_b	0.0445 ± 0.0004	0.0433 ± 0.0005	0.0440 ± 0.0005
Ω_c	$0.2563^{+0.0075}_{-0.0071}$	$0.2722^{+0.0100}_{-0.0096}$	$0.2634^{+0.0106}_{-0.0101}$
w_0	-1	$-1.2132^{+0.0654}_{-0.0659}$	$-1.0230^{+0.0692}_{-0.0626}$
w_a	0	$0.6415^{+0.3945}_{-0.3822}$	$0.6470^{+0.5976}_{-0.6253}$
γ	0	0	$-0.0078^{+0.0192}_{-0.0118}$

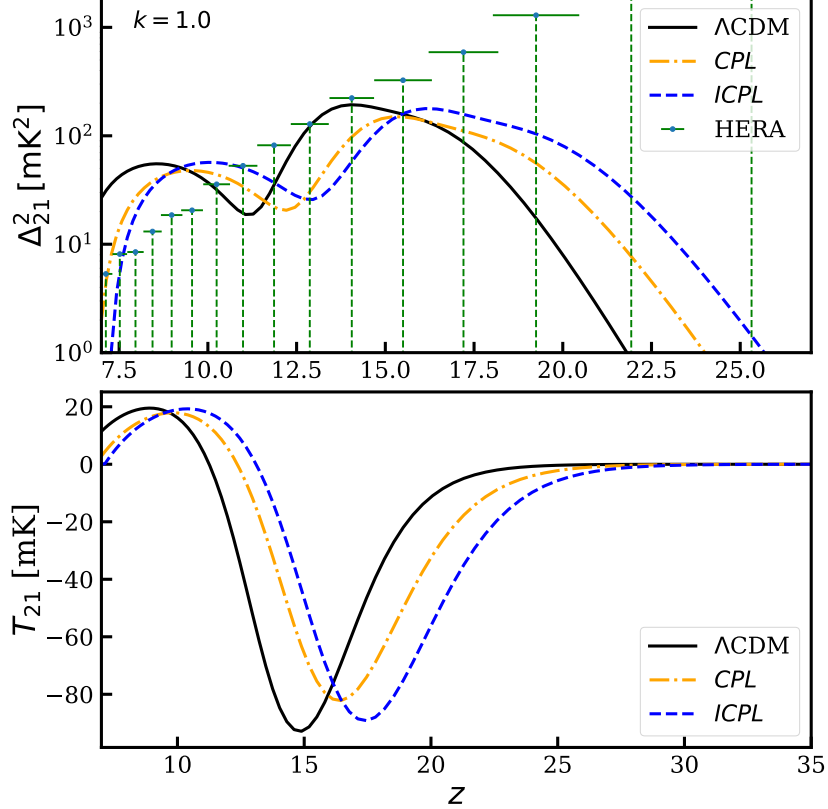


Figure 5: The power spectra (Δ_{21}^2) and brightness temperature (T_{21}) of the 21-cm signal. The theoretical value of the Λ CDM, the CPL, and the ICPL models are shown in the black line, yellow-dash line, and blue-dash line, respectively. In this figure, the wave number k is 1.0. The expected noise from HERA shows in green points.

IV. RESULT AND DISCUSSION

The three dark energy models above have been constrained by the previous research [33–36]. In this work, we are more interested in the evolution of the three models in the local Universe, so we fit free parameters by comparing the data from baryon acoustic oscillations (BAO) [63–66] and Type Ia supernovae (SNIa) [67, 68]. The best-fit results are shown in Tab. II. H_0 value from the model and the ICPL model are $70.6986^{+0.2639}_{-0.2601}$ km/s/Mpc and $70.9338^{+0.2549}_{-0.2515}$ km/s/Mpc. The fitting result of γ is a negative number $-0.0078^{+0.0192}_{-0.0118}$, which means that a high possibility of the energy transfer from dark matter to dark energy.

To get the 21-cm signal, we utilize the local SFRD method to derive correlation functions incorporating nonlinear effects [37]. The SFRD serves as the fundamental component for determining the statistics of radiative fields by the *Zeus21* program [37] combined with *CLASS* [69, 70]. From Eq. (5),

we have known the 21-cm line signal is influenced by various factors, including the temperature of the cosmic microwave background T_{CMB} , the kinetic temperature of the gas T_k , and the spin temperature T_S . From the evolution of these temperature components in Fig. 1, we find that the spin temperature and gas kinetic temperature in the CPL and ICPL models are higher than the Λ CDM at redshift $z \approx 10$. T_{CMB} is nearly the same in all three models, which is easy to understand that dynamic dark energy models primarily affect the Universe locally while having less impact on the CMB temperature.

The power spectrum of the primordial density perturbations can be described as

$$\Delta_{21}^2 = k^3 \frac{P_{21}(k)}{2\pi^2}. \quad (12)$$

$P_{21}(k)$ is the 21-cm power spectrum, which measures the amplitude of the brightness temperature fluctuations as a function of spatial scale. The quantity $\Delta_{21}^2(k)$ relates to the variance of the brightness temperature fluctuations on a given scale k as $\langle \delta T_b(\mathbf{k}) \delta T_b(\mathbf{k}') \rangle = (2\pi)^3 \delta_D(\mathbf{k} - \mathbf{k}') \Delta_{21}^2(k)$, where $\delta T_b(\mathbf{k})$ is the Fourier transform of the brightness temperature fluctuations, and $\delta_D(\mathbf{k})$ is the Dirac delta function.

We compare the Δ_{21}^2 of the three models in Fig. 2. The scale factor k in our setting is 0.1, 0.5, and 1.0, respectively. With these fixed values, we find that the power spectra increase with the value of k . At $k = 0.1 \text{ Mpc}^{-1}$, the power spectrum exhibits distinct features, characterized by two bumps from $z \geq 10$. The right bump corresponds to the epoch of coupling (EoC) which refers to the period when Lyman-alpha fluctuations dominate. During this epoch, the Lyman-alpha photons emitted by the first galaxies couple the spin temperature of neutral hydrogen to the kinetic temperature of the intergalactic medium (IGM) and this coupling is known as the WF effect. The left bump is the epoch of X-ray Heating (EoH). It is characterized by the influence of X-rays emitted by galaxies, which heat up the surrounding IGM and affect the 21-cm signal. Between the two eras, the negative contribution from the cross-power between these fields leads to relative troughs in the power spectrum. Compared with the Λ CDM, the peak and concave point of the bump were shifted to an earlier Universe in CPL and ICPL. Especially, the ICPL has a higher corresponding redshift than CPL, which shows that the interaction term makes the ICPL obtain a faster evolution of our Universe. At smaller scales ($k = 1.0 \text{ Mpc}^{-1}$), the peak of the bump in the Λ CDM is higher than the CPL and ICPL models. This is because the two models have smaller fluctuations in the 21-cm signal.

In Fig. 3, the power spectrum is shown at three specific redshifts. These 3 redshifts are chosen to represent different epoch slices in the Λ CDM: the EoH at $z = 12$, the EoC at $z = 17$, and the transition between EoH and EoC ($z = 15$). For $z = 12$ and $z = 17$, the power spectrum remains relatively flat with k . However, at the transition redshift of the Λ CDM, the power spectra experience a significant drop. This drop is caused by the negative contribution of cross-terms between the two physical processes.

Now, we plot the 21-cm power spectrum and the global brightness temperature of these three models with different wavenumber k in Fig. 4 and Fig. 5. For $k = 0.2$ in Fig. 4, the third bump appears at z around 9, which corresponds to the Epoch of Reionization (EoR). During this epoch, the first galaxies and quasars emit high-energy photons that ionize the neutral hydrogen in the intergalactic medium. As ionization spreads through the Universe, ionization fraction fluctuations become a dominant factor in shaping the 21-cm signal. The other bumps are the EoC and EoH, as discussed in Fig. 2 and Fig. 3. Same with the previous results, the bump peaks in CPL and ICPL models were shifted to the earlier Universe, which indicates the formation of the first stars and galaxies occurs at ICPL earlier than the CPL model, and even earlier than the Λ CDM.

The global 21-cm brightness temperature T_{21} confirmed this result, which the ICPL and CPL model enters every epoch earlier than the Λ CDM. The lowest point of the absorption trough in the 21-cm signal, characterized by a temperature of approximately -90 mK, is significantly shallower compared to the value claimed by the EDGES experiment, which is around -500 mK [1]. This significant discrepancy between the observations and the predicted signal has led to the exploration of alternative explanations. The ICPL has the potential to enlarge the signal in the theory, but this phenomenon still needs to consider additional physical processes to affect the evolution of the intergalactic medium and the 21-cm signal.

We also considered the expected noise level of observations in Fig. 5. It includes the expected noise level after 1 year (1080 hours) of integration with the HERA telescope shown in green points [71]. The noise calculation is performed using the *21cmSense* software [72, 73], assuming a moderate-foreground scenario with a buffer value of $a = 0.1 h \text{ Mpc}^{-1}$ above the horizon. The noise level provides an estimate of the sensitivity and precision of the measurements that can be achieved with HERA under these assumptions. In our study, we demonstrate that the significance of the three models can be detected

at redshift around $z \approx 10 - 15$. These features will help to distinguish the three models with more accurate observations in the future and will help us to distinguish the equation of state of dynamical dark energy.

V. SUMMARY

In this paper, we discussed the difference in the background evolution in the Λ CDM, the CPL model, and the ICPL model. The ICPL model was considered with an interaction term of the form $Q = 3\gamma H\rho_c$. We numerically compared the best-fit parameters obtained for the three models with Type Ia Supernovae and Baryon Acoustic Oscillations data, which are the local observations without being disturbed by the CMB. The result of γ is a negative number, that shows the energy transfer from dark matter to dark energy. These results were used in the calculation of 21-cm global signal.

We calculated the evolution of the CMB temperature T_{CMB} , kinetic temperature T_k , and spin temperature T_s in different cosmological models with the *Zeus21* and *CLASS* program. We found that T_{CMB} did not exhibit significant changes among the three models. However, the T_k and T_s values in the CPL and ICPL models were approximately twice as large as those in the Λ CDM. Moreover, we analyzed the 21-cm power spectra at various wave numbers k , to investigate the epoch of reionization, the epoch of X-ray heating, and the epoch of coupling in the three models. We found that these epochs in the CPL and ICPL models occurred at earlier redshifts due to the different expansion rates during cosmic dawn. The variations of bumps in the power spectra provided valuable information about the process of reionization.

We also plotted the brightness temperature of the 21-cm line of the three models. We found that the moment of the first galaxy formation and the epoch of reheating occurred earlier in CPL and ICPL models compared to the Λ CDM. Specifically, the ICPL model exhibited an even earlier onset than the CPL model. In our calculation, the ICPL model can help to relieve the tension about the lowest point of the absorption between the theoretical expectations and the strength of this signal reported by the EDGES experiment, which shows that the interacting dark energy model has the potential to get a lower T_{21} signal.

Furthermore, based on our analysis using HERA expected noise signal, we find that the features of the Λ CDM, the CPL, and the ICPL model have possibly to be detected with more accurate observation. This suggests that future observations with HERA have the potential to distinguish different dark energy models and their equations of state. The observation of 21-cm can provide valuable information on the nature of dark energy and the early Universe.

Acknowledgements

We thank Julian B. Muñoz for the useful discussion. LY was supported by the YST project in APCTP.

-
- [1] J. D. Bowman, A. E. E. Rogers, R. A. Monsalve, T. J. Mozdzen and N. Mahesh, *Nature* **555**, no.7694, 67-70 (2018) doi:10.1038/nature25792 [arXiv:1810.05912 [astro-ph.CO]].
 - [2] J. R. Pritchard and A. Loeb, *Rept. Prog. Phys.* **75**, 086901 (2012) doi:10.1088/0034-4885/75/8/086901 [arXiv:1109.6012 [astro-ph.CO]].
 - [3] M. F. Morales and J. S. B. Wyithe, *Ann. Rev. Astron. Astrophys.* **48**, 127-171 (2010) doi:10.1146/annurev-astro-081309-130936 [arXiv:0910.3010 [astro-ph.CO]].
 - [4] S. Furlanetto, S. P. Oh and F. Briggs, *Phys. Rept.* **433**, 181-301 (2006) doi:10.1016/j.physrep.2006.08.002 [arXiv:astro-ph/0608032 [astro-ph]].
 - [5] H. Tashiro, K. Kadota and J. Silk, *Phys. Rev. D* **90**, no.8, 083522 (2014) doi:10.1103/PhysRevD.90.083522 [arXiv:1408.2571 [astro-ph.CO]].
 - [6] C. Feng and G. Holder, *Astrophys. J. Lett.* **858**, no.2, L17 (2018) doi:10.3847/2041-8213/aac0fe [arXiv:1802.07432 [astro-ph.CO]].
 - [7] R. Barkana, N. J. Outmezguine, D. Redigolo and T. Volansky, *Phys. Rev. D* **98**, no.10, 103005 (2018) doi:10.1103/PhysRevD.98.103005 [arXiv:1803.03091 [hep-ph]].
 - [8] M. S. Mahdawi and G. R. Farrar, *JCAP* **10**, 007 (2018) doi:10.1088/1475-7516/2018/10/007 [arXiv:1804.03073 [hep-ph]].

- [9] J. Mirocha and S. R. Furlanetto, *Mon. Not. Roy. Astron. Soc.* **483**, no.2, 1980-1992 (2019) doi:10.1093/mnras/sty3260 [arXiv:1803.03272 [astro-ph.GA]].
- [10] A. Ewall-Wice, T. C. Chang, J. Lazio, O. Dore, M. Seiffert and R. A. Monsalve, *Astrophys. J.* **868**, no.1, 63 (2018) doi:10.3847/1538-4357/aae51d [arXiv:1803.01815 [astro-ph.CO]].
- [11] S. Hirano and V. Bromm, *Mon. Not. Roy. Astron. Soc.* **480**, no.1, L85-L89 (2018) doi:10.1093/mnrasl/sly132 [arXiv:1803.10671 [astro-ph.GA]].
- [12] T. Venumadhav, L. Dai, A. Kaurov and M. Zaldarriaga, *Phys. Rev. D* **98**, no.10, 103513 (2018) doi:10.1103/PhysRevD.98.103513 [arXiv:1804.02406 [astro-ph.CO]].
- [13] S. Clark, B. Dutta, Y. Gao, Y. Z. Ma and L. E. Strigari, *Phys. Rev. D* **98**, no.4, 043006 (2018) doi:10.1103/PhysRevD.98.043006 [arXiv:1803.09390 [astro-ph.HE]].
- [14] J. B. Muñoz, C. Dvorkin and A. Loeb, *Phys. Rev. Lett.* **121**, no.12, 121301 (2018) doi:10.1103/PhysRevLett.121.121301 [arXiv:1804.01092 [astro-ph.CO]].
- [15] M. Pospelov, J. Pradler, J. T. Ruderman and A. Urbano, *Phys. Rev. Lett.* **121**, no.3, 031103 (2018) doi:10.1103/PhysRevLett.121.031103 [arXiv:1803.07048 [hep-ph]].
- [16] C. Li and Y. F. Cai, *Phys. Lett. B* **788**, 70-75 (2019) doi:10.1016/j.physletb.2018.11.011 [arXiv:1804.04816 [astro-ph.CO]].
- [17] A. Hektor, G. Hütsi, L. Marzola and V. Vaskonen, *Phys. Lett. B* **785**, 429-433 (2018) doi:10.1016/j.physletb.2018.09.009 [arXiv:1805.09319 [hep-ph]].
- [18] C. Li, N. Houston, T. Li, Q. Yang and X. Zhang, *Int. J. Mod. Phys. D* **30**, no.06, 2150041 (2021) doi:10.1142/S0218271821500413 [arXiv:1812.03931 [hep-ph]].
- [19] S. Fraser, A. Hektor, G. Hütsi, K. Kannike, C. Marzo, L. Marzola, C. Spethmann, A. Racioppi, M. Raidal and V. Vaskonen, *et al.* *Phys. Lett. B* **785**, 159-164 (2018) doi:10.1016/j.physletb.2018.08.035 [arXiv:1803.03245 [hep-ph]].
- [20] Y. Yang, *Phys. Rev. D* **98**, no.10, 103503 (2018) doi:10.1103/PhysRevD.98.103503 [arXiv:1803.05803 [astro-ph.CO]].
- [21] G. D'Amico, P. Panci and A. Strumia, *Phys. Rev. Lett.* **121**, no.1, 011103 (2018) doi:10.1103/PhysRevLett.121.011103 [arXiv:1803.03629 [astro-ph.CO]].
- [22] A. Mitridate and A. Podo, *JCAP* **05**, 069 (2018) doi:10.1088/1475-7516/2018/05/069 [arXiv:1803.11169 [hep-ph]].
- [23] K. Cheung, J. L. Kuo, K. W. Ng and Y. L. S. Tsai, *Phys. Lett. B* **789**, 137-144 (2019) doi:10.1016/j.physletb.2018.11.058 [arXiv:1803.09398 [astro-ph.CO]].
- [24] R. Barkana, *Nature* **555**, no.7694, 71-74 (2018) doi:10.1038/nature25791 [arXiv:1803.06698 [astro-ph.CO]].
- [25] E. D. Kovetz, V. Poulin, V. Gluscevic, K. K. Boddy, R. Barkana and M. Kamionkowski, *Phys. Rev. D* **98**, no.10, 103529 (2018) doi:10.1103/PhysRevD.98.103529 [arXiv:1807.11482 [astro-ph.CO]].
- [26] T. R. Slatyer and C. L. Wu, *Phys. Rev. D* **98**, no.2, 023013 (2018) doi:10.1103/PhysRevD.98.023013 [arXiv:1803.09734 [astro-ph.CO]].
- [27] J. B. Muñoz and A. Loeb, *Nature* **557**, no.7707, 684 (2018) doi:10.1038/s41586-018-0151-x [arXiv:1802.10094 [astro-ph.CO]].
- [28] A. Berlin, D. Hooper, G. Krnjaic and S. D. McDermott, *Phys. Rev. Lett.* **121**, no.1, 011102 (2018) doi:10.1103/PhysRevLett.121.011102 [arXiv:1803.02804 [hep-ph]].
- [29] L. Xiao, R. An, L. Zhang, B. Yue, Y. Xu and B. Wang, *Phys. Rev. D* **99**, no.2, 023528 (2019) doi:10.1103/PhysRevD.99.023528 [arXiv:1807.05541 [astro-ph.CO]].
- [30] A. A. Costa, R. C. G. Landim, B. Wang and E. Abdalla, *Eur. Phys. J. C* **78**, no.9, 746 (2018) doi:10.1140/epjc/s10052-018-6237-7 [arXiv:1803.06944 [astro-ph.CO]].
- [31] Y. Wang and G. B. Zhao, *Astrophys. J.* **869**, no.1, 26 (2018) doi:10.3847/1538-4357/aaeb9c [arXiv:1805.11210 [astro-ph.CO]].
- [32] C. Li, X. Ren, M. Khurshudyan and Y. F. Cai, *Phys. Lett. B* **801**, 135141 (2020) doi:10.1016/j.physletb.2019.135141 [arXiv:1904.02458 [astro-ph.CO]].
- [33] M. Chevallier and D. Polarski, *Int. J. Mod. Phys. D* **10**, 213-224 (2001) doi:10.1142/S0218271801000822 [arXiv:gr-qc/0009008 [gr-qc]].
- [34] E. V. Linder, *Phys. Rev. Lett.* **90**, 091301 (2003) doi:10.1103/PhysRevLett.90.091301 [arXiv:astro-ph/0208512 [astro-ph]].
- [35] E. Ó. Colgáin, M. M. Sheikh-Jabbari and L. Yin, *Phys. Rev. D* **104**, no.2, 023510 (2021) doi:10.1103/PhysRevD.104.023510 [arXiv:2104.01930 [astro-ph.CO]].
- [36] J. H. He and B. Wang, *JCAP* **06**, 010 (2008) doi:10.1088/1475-7516/2008/06/010 [arXiv:0801.4233 [astro-ph]].
- [37] J. B. Muñoz, [arXiv:2302.08506 [astro-ph.CO]].
- [38] S. Singh, R. Subrahmanyam, N. U. Shankar, M. S. Rao, B. S. Girish, A. Raghunathan, R. Somashekar and K. S. Srivani, *Exper. Astron.* **45**, no.2, 269-314 (2018) doi:10.1007/s10686-018-9584-3 [arXiv:1710.01101 [astro-ph.IM]].
- [39] T. Peitzmann, C. Barlag, C. Blume, E. M. Bohne, D. Bucher, A. Claussen, R. Glasow, N. Heine, K. H. Kampert and R. Santo, *et al.* *Nucl. Instrum. Meth. A* **376**, 368-374 (1996) doi:10.1016/0168-9002(96)00224-0
- [40] M. P. van Haarlem, M. W. Wise, A. W. Gunst, G. Heald, J. P. McKean, J. W. T. Hessels, A. G. de Bruyn,

- R. Nijboer, J. Swinbank and R. Fallows, *et al.* *Astron. Astrophys.* **556**, A2 (2013) doi:10.1051/0004-6361/201220873 [arXiv:1305.3550 [astro-ph.IM]].
- [41] A. P. Beardsley, B. J. Hazelton, I. S. Sullivan, P. Carroll, N. Barry, M. Rahimi, B. Pindor, C. M. Trott, J. Line and D. C. Jacobs, *et al.* *Astrophys. J.* **833**, no.1, 102 (2016) doi:10.3847/1538-4357/833/1/102 [arXiv:1608.06281 [astro-ph.IM]].
- [42] S. J. Tingay, R. Goetze, J. D. Bowman, D. Emrich, S. M. Ord, D. A. Mitchell, M. F. Morales, T. Booler, B. Crosse and D. Pallot, *et al.* *Publ. Astron. Soc. Austral.* **30**, 7 (2013) doi:10.1017/pasa.2012.007 [arXiv:1206.6945 [astro-ph.IM]].
- [43] D. R. DeBoer, A. R. Parsons, J. E. Aguirre, P. Alexander, Z. S. Ali, A. P. Beardsley, G. Bernardi, J. D. Bowman, R. F. Bradley and C. L. Carilli, *et al.* *Publ. Astron. Soc. Pac.* **129**, no.974, 045001 (2017) doi:10.1088/1538-3873/129/974/045001 [arXiv:1606.07473 [astro-ph.IM]].
- [44] Z. Abdurashidova *et al.* [HERA], *Astrophys. J.* **924**, no.2, 51 (2022) doi:10.3847/1538-4357/ac2ffc [arXiv:2108.07282 [astro-ph.CO]].
- [45] M. G. Santos, P. Bull, D. Alonso, S. Camera, P. G. Ferreira, G. Bernardi, R. Maartens, M. Viel, F. Villaescusa-Navarro and F. B. Abdalla, *et al.* *PoS AASKA14*, 019 (2015) doi:10.22323/1.215.0019 [arXiv:1501.03989 [astro-ph.CO]].
- [46] J. F. Zhang, L. Y. Gao, D. Z. He and X. Zhang, *Phys. Lett. B* **799** (2019), 135064 doi:10.1016/j.physletb.2019.135064 [arXiv:1908.03732 [astro-ph.CO]].
- [47] Y. Xu and X. Zhang, *Sci. China Phys. Mech. Astron.* **63** (2020) no.7, 270431 doi:10.1007/s11433-020-1544-3 [arXiv:2002.00572 [astro-ph.CO]].
- [48] L. F. Wang, Y. Shao, G. P. Zhang, J. F. Zhang and X. Zhang, [arXiv:2201.00607 [astro-ph.CO]].
- [49] P. Hartley, A. Bonaldi, R. Braun, J. N. H. S. Aditya, S. Aicardi, L. Alegre, A. Chakraborty, X. Chen, S. Choudhuri and A. O. Clarke, *et al.* doi:10.1093/mnras/stad1375 [arXiv:2303.07943 [astro-ph.IM]].
- [50] R. Barkana and A. Loeb, *Phys. Rept.* **349**, 125-238 (2001) doi:10.1016/S0370-1573(01)00019-9 [arXiv:astro-ph/0010468 [astro-ph]].
- [51] R. Barkana and A. Loeb, *Astrophys. J.* **626**, 1-11 (2005) doi:10.1086/429954 [arXiv:astro-ph/0410129 [astro-ph]].
- [52] R. Barkana and A. Loeb, *Mon. Not. Roy. Astron. Soc.* **372**, L43-L47 (2006) doi:10.1111/j.1745-3933.2006.00222.x [arXiv:astro-ph/0512453 [astro-ph]].
- [53] Y. Mao, P. R. Shapiro, G. Mellema, I. T. Iliev, J. Koda and K. Ahn, *Mon. Not. Roy. Astron. Soc.* **422**, 926-954 (2012) doi:10.1111/j.1365-2966.2012.20471.x [arXiv:1104.2094 [astro-ph.CO]].
- [54] C. M. Hirata, *Mon. Not. Roy. Astron. Soc.* **367**, 259-274 (2006) doi:10.1111/j.1365-2966.2005.09949.x [arXiv:astro-ph/0507102 [astro-ph]].
- [55] R. G. Cai and A. Wang, *JCAP* **03**, 002 (2005) doi:10.1088/1475-7516/2005/03/002 [arXiv:hep-th/0411025 [hep-th]].
- [56] L. Amendola, G. Camargo Campos and R. Rosenfeld, *Phys. Rev. D* **75**, 083506 (2007) doi:10.1103/PhysRevD.75.083506 [arXiv:astro-ph/0610806 [astro-ph]].
- [57] M. Li, X. D. Li, S. Wang, Y. Wang and X. Zhang, *JCAP* **12**, 014 (2009) doi:10.1088/1475-7516/2009/12/014 [arXiv:0910.3855 [astro-ph.CO]].
- [58] Y. H. Li and X. Zhang, *Phys. Rev. D* **89**, no.8, 083009 (2014) doi:10.1103/PhysRevD.89.083009 [arXiv:1312.6328 [astro-ph.CO]].
- [59] C. Q. Geng, C. C. Lee and L. Yin, *JCAP* **08**, 032 (2017) doi:10.1088/1475-7516/2017/08/032 [arXiv:1704.02136 [astro-ph.CO]].
- [60] J. J. Zhang, L. Yin and C. Q. Geng, *Annals Phys.* **397**, 400-409 (2018) doi:10.1016/j.aop.2018.08.015 [arXiv:1809.04218 [astro-ph.CO]].
- [61] C. Q. Geng, C. C. Lee and L. Yin, *Eur. Phys. J. C* **80**, no.1, 69 (2020) doi:10.1140/epjc/s10052-020-7653-z [arXiv:2001.05092 [astro-ph.CO]].
- [62] C. Q. Geng, Y. T. Hsu, L. Yin and K. Zhang, *Chin. Phys. C* **44**, 105104 (2020) doi:10.1088/1674-1137/abab86 [arXiv:2002.05290 [astro-ph.CO]].
- [63] S. Alam *et al.* [BOSS], *Mon. Not. Roy. Astron. Soc.* **470**, no.3, 2617-2652 (2017) doi:10.1093/mnras/stx721 [arXiv:1607.03155 [astro-ph.CO]].
- [64] A. J. Ross *et al.* [BOSS], *Mon. Not. Roy. Astron. Soc.* **464**, no.1, 1168-1191 (2017) doi:10.1093/mnras/stw2372 [arXiv:1607.03145 [astro-ph.CO]].
- [65] M. Vargas-Magaña, S. Ho, A. J. Cuesta, R. O'Connell, A. J. Ross, D. J. Eisenstein, W. J. Percival, J. N. Grieb, A. G. Sánchez and J. L. Tinker, *et al.* *Mon. Not. Roy. Astron. Soc.* **477**, no.1, 1153-1188 (2018) doi:10.1093/mnras/sty571 [arXiv:1610.03506 [astro-ph.CO]].
- [66] F. Beutler *et al.* [BOSS], *Mon. Not. Roy. Astron. Soc.* **464**, no.3, 3409-3430 (2017) doi:10.1093/mnras/stw2373 [arXiv:1607.03149 [astro-ph.CO]].
- [67] D. M. Scolnic *et al.* [Pan-STARRS1], *Astrophys. J.* **859**, no.2, 101 (2018) doi:10.3847/1538-4357/aab9bb [arXiv:1710.00845 [astro-ph.CO]].
- [68] A. G. Riess, S. Casertano, W. Yuan, L. M. Macri and D. Scolnic, *Astrophys. J.* **876**, no.1, 85 (2019) doi:10.3847/1538-4357/ab1422 [arXiv:1903.07603 [astro-ph.CO]].
- [69] J. Lesgourgues, [arXiv:1104.2932 [astro-ph.IM]].
- [70] D. Blas, J. Lesgourgues and T. Tram, *JCAP* **07**, 034 (2011) doi:10.1088/1475-7516/2011/07/034

- [arXiv:1104.2933 [astro-ph.CO]].
- [71] J. B. Muñoz, Y. Qin, A. Mesinger, S. G. Murray, B. Greig and C. Mason, *Mon. Not. Roy. Astron. Soc.* **511**, no.3, 3657-3681 (2022) doi:10.1093/mnras/stac185 [arXiv:2110.13919 [astro-ph.CO]].
- [72] J. C. Pober, A. R. Parsons, D. R. DeBoer, P. McDonald, M. McQuinn, J. E. Aguirre, Z. Ali, R. F. Bradley, T. C. Chang and M. F. Morales, *Astron. J.* **145**, 65 (2013) doi:10.1088/0004-6256/145/3/65 [arXiv:1210.2413 [astro-ph.CO]].
- [73] J. C. Pober, A. Liu, J. S. Dillon, J. E. Aguirre, J. D. Bowman, R. F. Bradley, C. L. Carilli, D. R. DeBoer, J. N. Hewitt and D. C. Jacobs, *et al.* *Astrophys. J.* **782**, 66 (2014) doi:10.1088/0004-637X/782/2/66 [arXiv:1310.7031 [astro-ph.CO]].